Recent Advances in Small-Animal Cardiovascular Imaging

Benjamin M.W. Tsui and Dara L. Kraitchman

Russell H. Morgan Department of Radiology and Radiological Science, Johns Hopkins University School of Medicine, Baltimore, Maryland

Because of the development of gene knockout and transgenic technologies, small animals, such as mice and rats, have become the most widely used animals for cardiovascular imaging studies. Imaging can provide a method to serially evaluate the effect of a particular genetic mutation or pharmacologic therapy (*1*). In addition, imaging can be used as a noninvasive screening tool for particular cardiovascular phenotypes. Outcome measures of therapeutic efficacy, such as ejection fraction, left ventricular mass, and ventricular volume, can be determined noninvasively as well. Furthermore, small-animal imaging can be used to develop and test new molecular imaging probes (*2,3*). However, the small size of the heart and rapid heart rate of murine models create special challenges for cardiovascular imaging.

Key Words: molecular imaging; MI; animal imaging; cardiovascular; small animal

J Nucl Med 2009; 50:667–670
DOI: 10.2967/jnumed.108.058479

Although many challenges to small-animal cardiovascular imaging presently exist, the methods presented in this paper can be used as a noninvasive screening tool for particular cardiovascular phenotypes. In addition, small-animal imaging provides an economic platform for the rapid translation of new knowledge in cardiovascular medicine to the clinical arena.

CARDIAC MRI

Because of the small heart size and rapid heart rates in small animals such as mice and rats, most small-animal cardiac MRI has been performed on scanners with field strengths greater than 4.7-T. To minimize the effects of anesthetics on cardiac contractility, inhalational anesthesia—in combination with methods to maintain the animal's core temperature at 38°C—is used for MRI and other small-animal imaging modalities. As in clinical scanners, blurring due to cardiac motion is avoided by gating image acquisition to the electrocardiogram (ECG) and deriving a single image from several heart cycles. However, image acquisition time for multiple short- and long-axis views can result in 1 to several hours per animal. Obviously, this image acquisition time is not compatible with high-throughput screening of genetically manipulated mouse models. Several groups are exploring methods to image multiple mice simultaneously (*4–6*). To image multiple animals simultaneously, receiver coil arrays can be positioned over each animal or individual coils for each animal can be designed (*5,6*). Although parallel imaging techniques can be used to take advantage of individual receiver coil sensitivities and increase the speed of imaging, these systems are not often available or the software is lacking to implement such routine techniques on commercially available high-field small-animal scanners. One approach to enable the rapid translation of high-field small-animal techniques to the clinical realm is the marriage of a high-field 7-T MRI scanner with the clinical user interface and a high number of receiver channels. Figure 1 shows an example of black-blood cardiac MR images (*7*) using such a system and demonstrates the exquisite soft-tissue detail that can be obtained in the mouse. Another alternative is to develop specialized gradient inserts and receiver coils for small animals on clinical 1.5- and 3-T imaging platforms (*8*). Another approach to shorten acquisition time in multiple-mouse imaging is to acquire images without cardiac gating and retrospectively reconstruct the images on the basis of a separately acquired navigator or the image data itself (*4,9*). Imaging times can be reduced from several hours to a few minutes per imaging slice while simultaneously imaging several animals using such a wireless ECG approach.

For cell tracking using superparamagnetic iron oxides or perfusion imaging, moving to the higher field strengths used in small-animal imaging may not always be advantageous because of increased field inhomogeneity and artifacts caused by magnetic susceptibility effects such as the lung–heart or blood–tissue interfaces (*10*). However, higher field strengths have been advantageous for enhanced spatial resolution of the components of atherosclerotic plaques in combination with targeted contrast agents (*2,3*). A recent review by Nahrendorf et al. (*11*) provides more detail on these novel MRI molecular targets for cardiovascular MRI.

OPTICAL IMAGING

Optical imaging, like MRI, is beneficial because there is no exposure to ionizing radiation. Although techniques are under development for intravascular fluorescence imaging (*12*), most fluorescence imaging techniques have been performed ex vivo or as microscopic validation (*13*). One of the challenges of any optical imaging technique is the relatively shallow penetration of light-emitting probes due to photon scatter. As a result, these techniques are ideally suited for the imaging of small animals, where the light emission at the body surface can easily be detected. Anatomic imaging is provided by simple visible light camera systems. The introduction of commercially available systems for small-animal bioluminescence imaging (BLI) (*14*) that are relatively simple to

Received Nov. 24, 2008; revision accepted Feb. 24, 2009.
For correspondence or reprints contact: Benjamin M.W. Tsui, Johns Hopkins University School of Medicine, Russell H. Morgan Department of Radiology and Radiological Science, 601 N. Caroline St., Baltimore, MD 21287.
E-mail: tsui@jhmi.edu

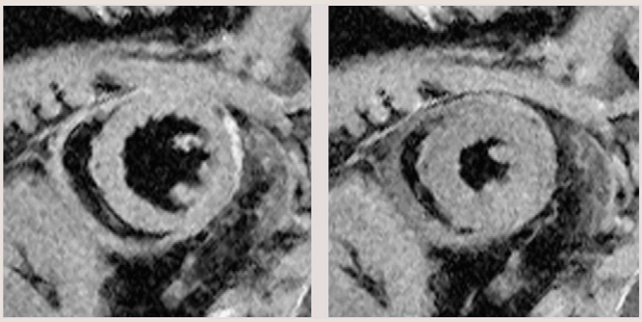

FIGURE 1. Representative short-axis end-diastolic (left) and end-systolic (right) images from 16–cardiac phase cine, black-blood imaging sequence in mouse using 7-T MRI scanner (spatial resolution of 0.1 × 0.1 × 1 mm) with a clinical user interface acquired in 4 min. Notice high contrast from ventricular cavity and myocardium that enables highly accurate measurement of left ventricular global function. Courtesy of Dr. Fred Epstein.

operate has resulted in a rapid expansion of these techniques for studying angiogenesis and cell tracking (*15,16*). Small-animal imaging systems have been developed to probe deeper in the body with tomographic fluorescent imaging (*17*). Although the BLI signal tends to be lower than fluorescent signals, the lack of background luminescence signal, compared with native tissue fluorescence, provides a slight advantage to in vivo BLI (*18*). Optical imaging techniques often rely on creating transfected cells to express a nonmammalian bioluminescence probe or introducing a probe that emits light when cleaved in the presence of a particular substrate, such as vascular cell adhesion molecule-1 or matrix metalloproteinases, which are both currently targets in the atherosclerotic plaque (*3,13,19*). Recently, Min et al. have demonstrated the BLI of cord blood mesenchymal stem cells transfected with a reporter gene expressing firefly luciferase to study the effects of immunosuppressive regimes on transplanted cell survival in the rat myocardium (*16*). One of the major benefits of a reporter gene technique for cell tracking is that only viable cells will be detected. We have recently demonstrated the combination of radiographic fluoroscopic imaging for the detection of encapsulated cells with BLI for the assessment of cell viability in a rabbit model of peripheral arterial disease (Fig. 2) (*20*).

CT

CT offers the ability to perform whole-body imaging with high anatomic detail. However, to achieve an image quality with CT comparable to that with a clinical system for in vivo small-animal imaging, a resolution of approximately 100 μm is required (*21,22*). Achieving this resolution requires some combination of increased dose or decreased ability to distinguish soft tissues (i.e., a decrease in contrast resolution), creating a unique challenge for small-animal micro-CT systems.

Micro-CT systems have been designed to rotate the radiographic or detector system around the animal, as is typically done in clinical systems. Most commercial micro-CT systems consist of a low-power radiographic tube of approximately 85 kVp and a flat-panel detector that acquires 2-dimensional (2D) projection images from multiple views around the animal. When imaging small live animals, these systems normally operate with an acquisition time on the order of several minutes and provide 3-dimensional (3D) volume images with a resolution of 100–200 μm. High-speed micro-CT for small-animal cardiovascular imaging is possible with a special high-power microfocus radiographic tube and a slip-ring gantry similar to that on human CT systems. This kind of system provides fast (~1–2 s) cardiovascular imaging at somewhat reduced resolutions (~200 μm) and increased radiation dose (*23*).

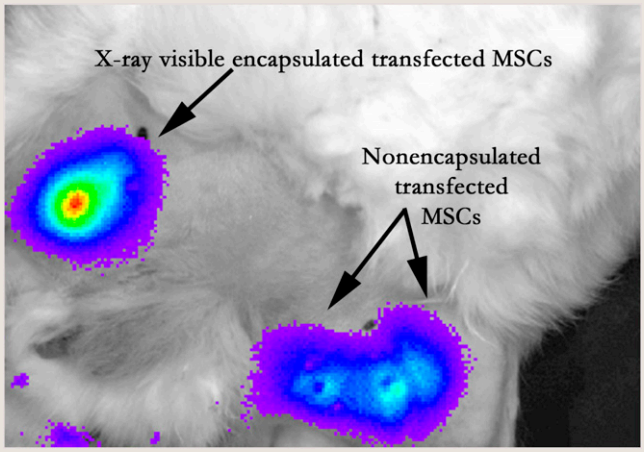

FIGURE 2. BLI after intramuscular injection in medial thigh of rabbit model of peripheral arterial disease provides ability to assess cell viability in vivo in radiography-visible encapsulated MSCs similar to that in nonencapsulated MSCs. Bioluminescence image was acquired in 60 s and overlaid on light image for anatomic delineation. MSCs = mesenchymal stem cells.

As with cardiac MRI, ECG gating strategies to freeze cardiac motion are used with micro-CT in cardiovascular imaging. In addition, traditional radiopaque contrast agents that are injected intravascularly to enhance contrast rapidly wash out of the blood pool and, thus, must be modified for micro-CT applications. A specialized lipid-emulsion contrast agent that has delayed uptake by hepatocytes (Fenestra VC; ART Advanced Research Technologies Inc.) and, therefore, remains intravascular for several hours has been developed for cardiovascular applications in micro-CT (*24,25*). Delayed-enhancement micro-CT has also been used to image myocardial infarction (*26*). However, most micro-CT studies use CT for anatomic localization typically in combination with radionuclide studies (Fig. 3).

RADIONUCLIDE IMAGING

Radionuclide imaging, one of the traditional imaging modalities, has received renewed interest as an important molecular imaging technique. By injecting a trace amount of biomarkers labeled with radioisotopes, radionuclide imaging allows the study of various myocardial functions and related diseases, including ejection fraction, regional wall motion

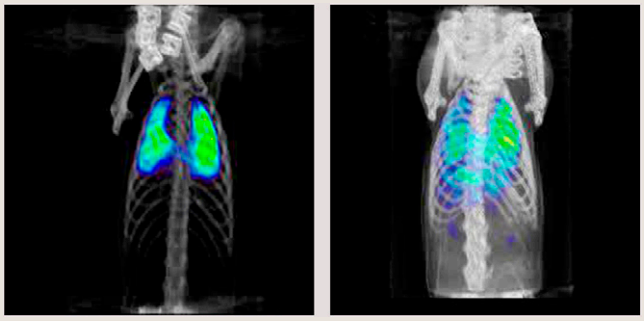

FIGURE 3. SPECT/CT rendering of ^{111}In-oxine radiolabeled MSCs (~2,886 kBq [~78 μCi] total activity) delivered intravenously to rat with doxyrubicine cardiotoxicity demonstrates initial high lung uptake (blue green on SPECT) immediately after injection (left), followed by redistribution to other organs at 24 h (right). MSCs = mesenchymal stem cells.

abnormalities, congestive heart failure, perfusion, viability, oxygen consumption, and glucose and fatty acid metabolism (*27–29*). Also, coronary artery functions and related diseases, such as ischemia, infarction, and atherosclerosis, can be investigated (*30–32*). In addition, because of its exceptional target specificity of radiotracers, radionuclide imaging allows imaging at the molecular level, such as receptor imaging (*33*), which cannot be accomplished by other imaging techniques.

Conventional radionuclide imaging uses a position-sensitive radiation detector, such as a scintillation or γ-camera, to detect the γ-ray photons emitting from the 3D distribution of radioactivity of the radiolabeled biomarker in vivo and form a 2D projection image. SPECT and PET apply image-reconstruction methods, which are based on mathematic formulations, to 2D projection images from multiple views and generate 3D images that represent the distribution of radioactivity in vivo in much higher image contrast and clarity than the 2D projection images.

During the past decade, significant advances have been made in detector technologies that provide much improved intrinsic resolution. The new technologies have been applied to clinical and small-animal SPECT and PET systems. In SPECT, using pinhole imaging geometry with magnification, both high resolution (on the order of 1 mm or less with small pinhole aperture and low photon energy) and high detection efficiency (on the order of 10^{-3} with a full-ring detector geometry and submillimeter resolution) can be achieved (*34,35*). For example, a unique line of multipinhole SPECT systems for small-animal imaging (U-SPECT-I and its commercial successor, U-SPECT-II) provide unprecedented resolution in mice of 350 μm for 0.35-mm pinholes and 450 μm for 0.6-mm pinholes. This system allows for the visualization of tracer uptake and retention in minute detail in the myocardium of the mouse, including the papillary muscle (Fig. 4) (*35,36*). Another advantage of small-animal SPECT is its ability to image multiple radiotracers that emit different energy photons simultaneously (*37*). By taking advantage of radionuclides with relatively long half-lives, small-animal SPECT has been used to track the migration of radiolabeled mesenchymal stem cells to myocardial infarction (*38*). Also, quantitative SPECT image-reconstruction methods with compensation for collimator-detector response, photon attenuation, and scatter that have been successfully applied to clinical SPECT (*39,40*) are becoming available to small-animal SPECT, for further improvement in image quality and quantitative accuracy (*41–43*).

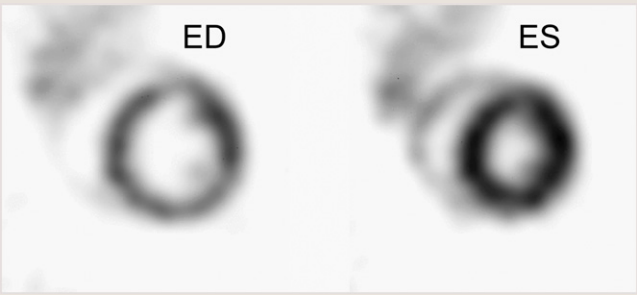

FIGURE 4. Sample ultra-high-resolution ^{99m}Tc-tetrofosmin SPECT images of heart of mouse in end-diastole (ED) and end-systole (ES), showing myocardial perfusion in minute detail in papillary muscles and right ventricular wall. Male C57BL/6 mouse (30 g) was injected intravenously with 190 MBq of ^{99m}Tc-tetrofosmin and anesthetized using ketamine, medetomidine, and atropine. At 45 min after injection, mouse was imaged for 1 h using U-SPECT-II system with 0.6-mm-diameter pinhole inserts. During image acquisition, an ECG trigger signal was acquired (BioVet; m2m Imaging) and incorporated in list-mode data. A 16-gate reconstruction was performed. Image data courtesy of Freek J. Beekman.

The 511-keV high-energy photons, effective range of energetic positrons (e.g., from 0.2 mm for ^{18}F to ~2.6 mm for ^{82}Rb), and small noncolinearity between the 2 annihilation 511-keV photons become limiting factors for high-resolution small-animal PET (*44,45*). Current small-animal PET systems have a spatial resolution of 1.5 mm and detection efficiency on the order of a few percent (*46,47*). The main advantages of PET include its higher detection efficiency and the availability of positron-emitting radionuclides, including ^{11}C, ^{13}N, ^{15}O, and ^{18}F, which allows the labeling of many physiologically and biochemically interesting biomarkers that are involved in health and disease (*48*). Three-dimensional quantitative image-reconstruction methods with compensation for detector response, photon attenuation, and scatter have also been applied to small-animal PET for further improvement in image quality of quantitative accuracy (Fig. 5) (*49,50*).

Although small-animal SPECT and PET images offer unique functional information at the molecular level, they are often difficult to interpret because of the lack of correlation with anatomic structures or biologic landmarks. Because CT images provide excellent anatomic information, multimodality SPECT/CT and PET/CT have become standard clinical and small-animal molecular imaging systems (*51*). More recently, trimodality preclinical small-animal systems with SPECT/PET/CT are becoming commercially available. Also, because of the anatomic information, soft-tissue differentiation, and additional functional information offered by coregistered MR images, dual-modality clinical and preclinical small-animal SPECT/MRI (*52*) and PET/MRI (*53*) systems are under active research and development.

Because of the availability of commercial radiolabeled tracers, preclinical molecular imaging using radionuclide techniques has enjoyed much progress. At the same time, fueled by advances in the development of new radiomarkers and radiopharmaceuticals, radionuclide imaging including SPECT and PET has become increasingly important in the preclinical molecular imaging of cardiovascular functions and diseases. Because success in preclinical molecular radionuclide imaging techniques can be directly translated to clinical studies, these methods are particularly important in drug development and translation medicine from in vitro to clinical practice.

CONCLUSION

Although many challenges to small-animal cardiovascular imaging presently exist, whole-body imaging allows the testing of new therapies in relevant disease models to study the safety and efficacy with outcome measures of promising agents similar to those that will be found in future clinical trials. In addition, genetically modified animals allow us to probe the underlying mechanisms of disease development and response to

FIGURE 5. Same single whole-body transaxial section from ^{18}F-FDG mouse study (26-g mouse, ~11.1 MBq [0.3 mCi] injected). Data were acquired using commercial small-animal PET system over 30 min, about 1 h after injection, and reconstructed with 3 different methods: Fourier rebinning (FORE)/filtered backprojection, FORE/2D ordered-subset expectation maximization (OS-EM), and 3D OS-EM. RV myocardium and intensely labeled LV myocardium are seen in all 3 ^{18}F-FDG reconstructions. FBP = filtered backprojection.

specific treatments that could enable the identification of potential new therapies or molecular imaging probes. Thus, small-animal imaging provides an economic platform for the rapid translation of new knowledge in cardiovascular medicine to the clinical arena.

ACKNOWLEDGMENT

This work was supported in part by the National Institutes of Health under grants R01-EB01558, U24-CA092871, R21-HL89029, R01-EB007825, and 2008 MSCRFII-0399-00 (MD Stem Cell Research Fund).

REFERENCES

1. Contag PR. Whole-animal cellular and molecular imaging to accelerate drug development. *Drug Discov Today.* 2002;7:555–562.
2. Lancelot E, Amirbekian V, Brigger I, et al. Evaluation of matrix metalloproteinases in atherosclerosis using a novel noninvasive imaging approach. *Arterioscler Thromb Vasc Biol.* 2008;28:425–432.
3. Nahrendorf M, Sosnovik DE, Weissleder R. MR-optical imaging of cardiovascular molecular targets. *Basic Res Cardiol.* 2008;103:87–94.
4. Esparza-Coss E, Ramirez MS, Bankson JA. Wireless self-gated multiple-mouse cardiac cine MRI. *Magn Reson Med.* 2008;59:1203–1206.
5. Ramirez MS, Bankson JA. A practical method for 2D multiple-animal MRI. *J Magn Reson Imaging.* 2007;26:1162–1166.
6. Ramirez MS, Ragan DK, Kundra V, Bankson JA. Feasibility of multiple-mouse dynamic contrast-enhanced MRI. *Magn Reson Med.* 2007;58:610–615.
7. Berr SS, Roy RJ, French BA, et al. Black blood gradient echo cine magnetic resonance imaging of the mouse heart. *Magn Reson Med.* 2005;53:1074–1079.
8. Gilson WD, Kraitchman DL. Cardiac magnetic resonance imaging in small rodents using clinical 1.5 T and 3.0 T scanners. *Methods.* 2007;43:35–45.
9. Larson AC, Kellman P, Arai A, et al. Preliminary investigation of respiratory self-gating for free-breathing segmented cine MRI. *Magn Reson Med.* 2005;53:159–168.
10. Farrar CT, Dai G, Novikov M, et al. Impact of field strength and iron oxide nanoparticle concentration on the linearity and diagnostic accuracy of off-resonance imaging. *NMR Biomed.* 2008;21:453–463.
11. Nahrendorf M, Sosnovik D, French B, et al. Multimodality cardiovascular molecular imaging, part II. *Circ Cardiovascr Imaging.* 2009;2:56–70.
12. Zhu B, Jaffer FA, Ntziachristos V, Weissleder R. Development of a near infrared fluorescence catheter: operating characteristics and feasibility for atherosclerotic plaque detection. *J Phys D Appl Phys.* 2005;38:2701–2707.
13. Tsourkas A, Shinde-Patil VR, Kelly KA, et al. In vivo imaging of activated endothelium using an anti-VCAM-1 magnetooptical probe. *Bioconjug Chem.* 2005;16:576–581.
14. Contag PR, Olomu IN, Stevenson DK, Contag CH. Bioluminescent indicators in living mammals. *Nat Med.* 1998;4:245–247.
15. Lin Y, Molter J, Lee Z, Gerson SL. Bioluminescence imaging of hematopoietic stem cell repopulation in murine models. *Methods Mol Biol.* 2008;430:295–306.
16. Min JJ, Ahn Y, Moon S, et al. In vivo bioluminescence imaging of cord blood derived mesenchymal stem cell transplantation into rat myocardium. *Ann Nucl Med.* 2006;20:165–170.
17. Zacharakis G, Ripoll J, Weissleder R, Ntziachristos V. Fluorescent protein tomography scanner for small animal imaging. *IEEE Trans Med Imaging.* 2005;24:878–885.
18. Troy T, Jekic-McMullen D, Sambucetti L, Rice B. Quantitative comparison of the sensitivity of detection of fluorescent and bioluminescent reporters in animal models. *Mol Imaging.* 2004;3:9–23.
19. Sosnovik DE, Windsor S, Nahrendorf M, et al. Tomographic fluorescence and MR imaging of myocardial inflammation in the beating mouse heart in vivo [abstract]. *J Cardiovasc Magn Reson.* 2006;8:85–86.
20. Kedziorek D, Walczak P, Azene N, Kraitchman DL. Cell visibility and viability assessment with novel bioluminescence assay of x-ray-visible microencapsulated mesenchymal stem cells. Paper presented at: 2008 World Molecular Imaging Conference; September 10–13, 2008; Nice, France.
21. Ritman EL. Small-animal CT: its difference from, and impact on, clinical CT. *Nucl Instrum Methods Phys Res A.* 2007;580:968–970.
22. Ford NL, Thornton MM, Holdsworth DW. Fundamental image quality limits for microcomputed tomography in small animals. *Med Phys.* 2003;30:2869–2877.
23. Ross W, Cody DD, Hazle JD. Design and performance characteristics of a digital flat-panel computed tomography system. *Med Phys.* 2006;33:1888–1901.
24. Weichert JP, Lee FT Jr, Longino MA, Chosy SG, Counsell RE. Lipid-based blood-pool CT imaging of the liver. *Acad Radiol.* 1998;5(suppl 1):S16–S19.
25. Badea CT, Drangova M, Holdsworth DW, Johnson GA. In vivo small-animal imaging using micro-CT and digital subtraction angiography. *Phys Med Biol.* 2008;53:R319–R350.
26. Nahrendorf M, Badea C, Hedlund LW, et al. High-resolution imaging of murine myocardial infarction with delayed-enhancement cine micro-CT. *Am J Physiol Heart Circ Physiol.* 2007;292:H3172–H3178.
27. Constantinesco A, Choquet P, Monassier L, Israel-Jost V, Mertz L. Assessment of left ventricular perfusion, volumes, and motion in mice using pinhole gated SPECT. *J Nucl Med.* 2005;46:1005–1011.
28. Lahoutte T. Monitoring left ventricular function in small animals. *J Nucl Cardiol.* 2007;14:371–379.
29. Vanhove C, Lahoutte T, Defrise M, Bossuyt A, Franken PR. Reproducibility of left ventricular volume and ejection fraction measurements in rat using pinhole gated SPECT. *Eur J Nucl Med Mol Imaging.* 2005;32:211–220.
30. Liu Z, Kastis GA, Stevenson GD, et al. Quantitative analysis of acute myocardial infarct in rat hearts with ischemia-reperfusion using a high-resolution stationary SPECT system. *J Nucl Med.* 2002;43:933–939.
31. Acton PD, Thomas D, Zhou R. Quantitative imaging of myocardial infarct in rats with high resolution pinhole SPECT. *Int J Cardiovasc Imaging.* 2006;22:429–434.
32. Tsui BMW, Wang YC, Qi YJ, et al. Feasibility of microSPECT/CT imaging of plaques in a transgenic mouse model. In: Kupinski M, Barrett H, eds. *Small Animal SPECT Imaging.* New York, NY: Springer; 2005:215–223.
33. Acton PD, Choi SR, Plossl K, Kung HF. Quantification of dopamine transporters in the mouse brain using ultra-high resolution single-photon emission tomography. *Eur J Nucl Med Mol Imaging.* 2002;29:691–698.
34. Beekman F, van der Have F. The pinhole: gateway to ultra-high-resolution three-dimensional radionuclide imaging. *Eur J Nucl Med Mol Imaging.* 2007;34:151–161.
35. Beekman FJ, van der Have F, Vastenhouw B, et al. U-SPECT-I: a novel system for submillimeter-resolution tomography with radiolabeled molecules in mice. *J Nucl Med.* 2005;46:1194–1200.
36. Vastenhouw B, Beekman F. Submillimeter total-body murine imaging with U-SPECT-I. *J Nucl Med.* 2007;48:487–493.
37. Siebelink HM, Natale D, Sinusas AJ, Wackers FJ. Quantitative comparison of single-isotope and dual-isotope stress-rest single-photon emission computed tomographic imaging for reversibility of defects. *J Nucl Cardiol.* 1996;3:483–493.
38. Kraitchman DL, Tatsumi M, Gilson WD, et al. Dynamic imaging of allogeneic mesenchymal stem cells trafficking to myocardial infarction. *Circulation.* 2005;112:1451–1461.
39. Tsui BMW, Zhao XD, Frey EC, McCartney WH. Quantitative single-photon emission computed tomography: basics and clinical considerations. *Semin Nucl Med.* 1994;24:38–65.
40. Tsui BMW. Quantitative SPECT. In: Henkin RE, Boles M, Dillehay GL, et al., eds. *Nuclear Medicine.* 2nd ed. Philadelphia, PA: Mosby Elsevier; 2006:223–245.
41. Hwang AB, Hasegawa BH. Attenuation correction for small animal SPECT imaging using x-ray CT data. *Med Phys.* 2005;32:2799–2804.
42. Tsui BMW, Wang YC. High-resolution molecular imaging techniques for cardiovascular research. *J Nucl Cardiol.* 2005;12:261–267.
43. van der Have F, Vastenhouw B, Rentmeester M, Beekman FJ. System calibration and statistical image reconstruction for ultra-high resolution stationary pinhole SPECT. *IEEE Trans Med Imaging.* 2008;27:960–971.
44. Cherry SR. In vivo molecular and genomic imaging: new challenges for imaging physics. *Phys Med Biol.* 2004;49:R13–R48.
45. Lecomte R. Technology challenges in small animal PET imaging. *Nucl Instrum Methods Phys Res A.* 2004;527:157–165.
46. Tai Y-C, Ruangma A, Rowland D, et al. Performance evaluation of the microPET Focus: a third-generation microPET scanner dedicated to animal imaging. *J Nucl Med.* 2005;46:455–463.
47. Wang Y, Seidel J, Tsui BMW, Vaquero JJ, Pomper MG. Performance evaluation of the GE Healthcare eXplore VISTA dual-ring small-animal PET scanner. *J Nucl Med.* 2006;47:1891–1900.
48. Lecomte R, Croteau E, Gauthier ME, et al. Cardiac PET imaging of blood flow, metabolism, and function in normal and infarcted rats. *IEEE Trans Nucl Sci.* 2004;51:696–704.
49. Johnson CA, Seidel J, Carson RE, et al. Evaluation of 3D reconstruction algorithms for a small animal PET camera. *IEEE Trans Nucl Sci.* 1997;44:1303–1308.
50. Qi J, Leahy RM, Cherry SR, Chatziioannou A, Farquhar TH. High-resolution 3D Bayesian image reconstruction using the microPET small-animal scanner. *Phys Med Biol.* 1998;43:1001–1013.
51. Hasegawa BH, Iwata K, Wong KH, et al. Dual-modality imaging of function and physiology. *Acad Radiol.* 2002;9:1305–1321.
52. Breton E, Choquet P, Goetz C, et al. Dual SPECT/MR imaging in small animal. *Nucl Instrum Methods Phys Res A.* 2007;571:446–448.
53. Zaidi H, Mawlawi O, Orton CG. Simultaneous PET/MR will replace PET/CT as the molecular multimodality imaging platform of choice. *Med Phys.* 2007;34:1525–1528.